A-7

Modified Magnetism at Buried Co/Pd Interface: Depth-Resolved Magnetic Circular Dichroism Study using Soft X-ray Standing Waves

Sang-Koog Kim* and J. B. Kortright

Materials Sciences Division, Lawrence Berkeley National Laboratory, University of California, One Cyclotron Road, Berkeley, California 94720, USA

Sung-Chul Shin

Department of Physics and Center for Nanospinics of Spintronic Materials, Korea Advanced Institute of Science and Technology, Taejon 305-701, Korea

Abstract

Soft x-ray standing waves produced by a multilayer interference substrate add depth-sensitivity to magnetic circular dichroism to resolve changes in Co magnetism across a 10 Å distance from the Co center to the Co-Pd interface of a Pd/Co/Pd trilayer having in-plane magnetization. Large enhancements of in-plane orbital and spin magnetic moments, as well as the number of *d* holes, are strongly localized in a thin interface layer. These results provide new insight into the phenomenon of magnetic anisotropy at buried interfaces, and suggest a broad applicability of such standing wave measurements to interface magnetism studies.

Interface magnetism is at the heart of much current magnetic research, driven by the discovery of new magnetic phenomena associated with interfaces, e.g., giant magnetoresistance and perpendicular magnetic anisotropy (PMA) and the realization of sophisticated measuring techniques and synthetic methods for layered structures [1-9]. Since PMA was observed in sputtered Co/Pd multilayer films [2], much experimental [3,4,7,10-14] and theoretical [15-19] work has focused on understanding its origin. This basic knowledge is important since it allows the engineering of films with desired magnetic anisotropy (MA) properties, such as better recording media using PMA to yield smaller magnetic bits and larger storage densities needed for massive data storage in the 21st century.

The behavior of measured MA as a function of thickness, t, of magnetic layers in Co-based multilayer systems has been found to vary apparently as $1/t$. Observed PMA at extremely small thicknesses is thus described by $K_{tot} = K_v + 2K_s/t$ [20]. Here K_v and K_s are the volume and interface contributions, respectively, to the total magnetic anisotropy constant, K_{tot}. K_s and K_v are generally considered to be intrinsic properties independent of t. It is believed that PMA occurs when a positive K_s

* To whom all correspondence should be addressed. E-mail:sangkoog@kaist.ac.kr.
Current Address: Department of Physics and Center for Nanospinics of Spintronic Materials, Korea Advanced Institute of Science and Technology, Taejon 305-701, Korea.

overcomes a negative K_v favoring in-plane magnetization by dipole-dipole interaction through shape anisotropy as t decreases. Studies of K_s typically utilize samples with different or varying t, since most experimental techniques lack depth resolution at buried interfaces [2-4,10,11]

Several structural origins have been considered as competing or cooperative sources of PMA, such as Néel's surface magnetocrystalline anisotropy (MCA) [1] and magnetoelastic anisotropy (MEA) by misfit strain [3,4,10-13]. However links between observed PMA showing $1/t$ dependence and possible explanations are intricately entwined and complicated by possible disorder at real interfaces in the form of chemical intermixing and lattice misfit strains [13,14]. There is no doubt that PMA is characteristic of interfaces of layers a few Å thick and hence that the values of K_s and K_v are ultimately controlled by the atomic-scale details of how the transition is made at the interface, including asymmetry of the chemical environment and subsequent lattice relaxation that influence electronic structure. Care must thus be taken in inferring changing interface and electronic structures with t. Probes that can resolve changes in magnetic properties over a few atomic layers from the interface to the center of a buried ultrathin magnetic layer are needed to better understand issues surrounding the origin of PMA. Such a probe, x-ray magnetic circular dichroism (MCD) with standing wave (SW) excitation, is developed and applied to the example Pd/Co/Pd system in this work.

MCD and the powerful sum rules connected with it [21,22] have been used in many previous studies to separately quantify spin and orbital moments and their anisotropy with element specificity [7,8,24,25]. Together these experimental and theoretical studies [15-19] offer new insight into the microscopic origin of PMA of ultrathin layered films. The orbital magnetic moment, m_l, and its anisotropy have been inferred from comparative measurements of ultrathin films of different or varying thickness, as K_s is measured versus t [7,26-29]. These MCD measurements typically average over 10-30 Å into the sample, and the interface moments are assumed not to change upon adding additional layers. MCD experiments have yet to clearly resolve changes in m_l and spin magnetic moment, m_s, across a given Co interface in the absence of complicating factors such as changes in interface structure with t and uncertainty in the directions of m_l and m_s.

In the present study, we have markedly improved the depth resolution of MCD, from the center of a 20- Å-thick Co layer to its interface with a Pd layer by using soft x-ray standing waves (SW) [30-32] generated by a nonmagnetic multilayer interference substrate, hereafter called the standing wave generator (SWG) (Fig. 1(a)). The SWG consisted of 40 repeating bilayers of W and B_4C, denoted as [W(20 Å)/B_4C(20 Å)]$_{40}$. As the incident angle, θ, or scattering vector, $q = 4\pi \sin\theta / \lambda_{x-ray}$ is scanned across the multilayer Bragg peak (Fig. 1(b)), the SW phase changes by π with respect to the period. The strong SW produced by the interference of incident and reflected fields near the Bragg peak extends outward through the trilayer overstructure, Pd(20 Å)/Co(20 Å)/Pd(10 Å)/vacuum, as shown in Fig. 1(c). The SW field intensity, $E^2(z)$, thus

modulates the helicity-dependent absorption in depth z, providing a means to depth-resolve the MCD spectra of the ultrathin Co layer.

X-ray reflectivity measurements of magnetron-sputtered SWG and SWG/trilayer samples yield the SWG period of 38.9 Ă and a 3 Ă interface roughness as derived from a static Debye-Waller model. Rutherford backscattering and x-ray fluorescence values for Co and Pd mass/area correspond to polycrystalline trilayer thickness of Pd(20.8 Ă)/Co(19.1 Ă)/Pd(10.4 Ă). The SWG/trilayer sample has an easy orientation of overall magnetization lying in the film plane, a coercivity of about 160 Oe, and more than 90 percent remanent magnetization from in-plane hysteresis loop measured up to 2 kOe magnetic field.

X-ray absorption data were measured using total electron yield (TEY) via sample drain current [33] in an applied magnetic field of +/- 1 kOe oriented parallel with the x ray propagation vector of out-of-plane elliptical polarization which had a measured degree of circular polarization of P_C=0.76. θ-scans across the SW resonance with reversed field direction at many fixed photon energies, $h\nu$, spanning the Co $L_{2,3}$ edges comprise the bulk of the data. $h\nu$-scans at fixed θ far from the Bragg peak provide reference absorption spectra to aid in normalizing the θ-scans to the $(q,h\nu)$ surfaces for opposite helicities in Fig. 2(a) and (b). These absorption surfaces show clear SW modulations around q = 0.17 $Å^{-1}$ corresponding to approximately the Bragg condition of the SWG. Distinct differences with helicity are observed at the Co $L_{2,3}$ edges that provide the SW-modulated MCD spectra of interest. Also observed is a background SW modulation with no helicity dependence from the nonmagnetic part of the sample.

Normalization of the absorption surfaces for each helicity proceeds by treating $h\nu$ spectra at fixed q corresponding to fixed SW position. Model calculations of $E^2(z,q,h\nu,helicity)$ for the entire SWG/trilayer structure using measured Co optical constants for different helicity and tabulated optical constants for other constituents aid in this normalization. The pre-edge modulation primarily due to the TEY of the Pd layers is subtracted at each q. Co absorption signals are then normalized to a per atom basis by dividing by the post-edge signals. The $h\nu$-dependence of Pd and Co signals due to the perturbation of the SW by the trilayer is calculated and corrected by scaling each of these calculations to the pre-edge signals before pre-edge background subtraction. Spin polarization of Pd by the Co layer is expected [26], but is not measured in this study. More details of this analysis will be reported elsewhere [34].

Polarization-averaged absorption spectra and Co MCD spectra obtained from normalized helicity-dependent Co absorption spectra (seen in cover figure) corrected for P_C and projected onto the film plane are shown in Fig. 2(c) and (d), respectively. The normalization procedure removes the q-dependent intensity effects of integrated $E^2(z)$ over the Co layer so that changes in these spectra with q should reveal changes in electronic and magnetic structures with depth across the Co layer. There is no direct transformation from q to z, and depth-resolving changes with q require the use of the calculations in Fig. 1. Depth resolution is primarily obtained when a strong SW exists,

namely in the range $0.16 < q < 0.18$ Å^{-1}, since outside of this range no strong enhancement of absorption with depth occurs (cf. Fig. 1(b)) and the entire Co layer contributes equally (aside from electron escape depth considerations). Thus, at q=0.17 Å^{-1}, the strong SW significantly enhances absorption from the Co atoms at the Co-Pd interface, as compared to a weaker SW enhancement at q=0.16 Å^{-1} at the center of the Co layer. Comparing results at these two q values thus resolves changes in Co absorption over just 10 Å, with some residual smearing due to the finite extent of the SW in z.

Using orbital and spin sum rules [21,22], m_L, m_S and the number of d holes, n_h are determined from integrated areas of the L_3 and L_2 peaks in the MCD and polarization-averaged spectra. Because of a potentially considerable, but unknown, dipole term at the interface [35], the pure m_S is not determined but rather the effective spin moment m_{Se}. Possible variations in n_h with depth are important because evaluating m_L and m_S requires known values of n_h. Variation in n_h is determined from changes in total area of polarization-averaged L_3 and L_2 lines, assuming that the radial dipole matrix element remains constant across the Co layer [25,26].

Applying these rules to our data shows large changes in n_h, m_L, m_{Se}, and m_L / m_{Se} versus q as displayed in Fig. 3. These are resolved in depth with the aid of $E^2(q)$ shown in Fig. 1(b). The increase in n_h at the interface, i.e., for q = 0.17 Å^{-1} is about 0.8 compared to its value at the center of the Co layer. This significant increase is unmistakable evidence for a modified Co spin-averaged electronic structure at the interface, whose origin can be considered from different perspectives. From the viewpoint of intermetallic bonding, this increase implies charge transfer from Co to Pd at either sharp or diffused interfaces. From the view of band structure, it implies a shift of the spin-averaged Co d-states upward in energy through interaction with Pd, resulting in a larger density above the Fermi level to yield the increased absorption.

Both m_L and m_{Se} show significant enhancements at the interface as compared to just 10 Å away at the Co layer center. m_L is enhanced from 0. 16 to 0.5 μ_B while m_S is enhanced by less than 20 percent [38]. The ratio m_L / m_{Se} shows a clear enhancement at the interface. The enhanced value, m_L=0.5 μ_B is the largest measured orbital enhancement among those reported; values reported to date may be less than the true interfacial values because of limited depth resolution. We expect that interfaces such as Co/Pd studied here exhibit disorder in the form of misfit strains and chemical intermixing [13,14]. While theories generally do not account for such disorder, these experimental results are in close agreement with theoretical predictions assuming ideal interfaces [19].

Both the large size and in-plane direction of the interfacial enhancement of m_L are significant. The size generally results from the redistribution of Co 3d electrons in the interfacial atoms that is expected both from the increase in n_h and from the changing average local environment of Co atoms at the interface. To the extent that

hybridization between Co $3d$ and Pd $4d$ states occurs [28,36], the spin-orbit coupling, ξ, of interfacial Co atoms may be increased by the 3-times larger ξ_{Pd-4d} [37]. These factors must contribute to the size of the m_L.

While it is impossible to measure the SW enhancement of $m_L^{\perp}$ perpendicular to the layers, all evidence suggests that this $m_L^{\perp}$ is no larger than measured in-plane $m_L^{\parallel}$ so that anisotropy in interfacial m_L is in-plane. Above coercivity the in-plane hysteresis loop shows almost complete saturation, with no indication of $m_L^{\perp}$ greater than $0.5\,\mu_B$ at interface. This is consistent with the result that an anisotropy of m_L is necessary for MCA [7,39]. The largest reported values of $m_L^{\perp}$ from Co/Pd multilayers exhibiting PMA are less than 0.3 μ_B [23,36], smaller than the interfacial $m_L^{\parallel}$ observed here. Results here suggest that enhanced interfacial m_L need not coincide with interface PMA as is generally predicted by Néel-type surface MCA. As PMA sets in with decreasing t, a change in m_L anisotropy from in-plane to perpendicular can occur. This indicates directly that K_S depends strongly on t, changing sign in the transition from in-plane MA to PMA.

Models for PMA should include the possibility of interfacial disorder such as chemical intermixing and positional disorder resulting from misfit strains. Both exist at interfaces in Co/Pd multilayers which exhibit transition layers 1 or 2 monolayers thick [13,14]. As t decreases, the transition layers on either side will eventually coalesce, yielding an ultrathin Co-rich, alloy-like layer. The strain and chemical symmetries of this 2-D alloy-like layer are different from those in the interfacial transition layers of thicker Co films, since one mediates the transition from Pd to Pd and the other from Pd to Co. We hypothesize that the transition to PMA coincides with the coalescence of these transition layers. The interface enhancements observed in this study clearly pertain to a transition layer between Pd and bulk-like Co, supporting this general model. In this model neither K_S nor K_V are necessarily intrinsic properties independent of t, especially in the ultrathin regime.

The transition to PMA represents a reorientation that ultimately must have a structural origin since anisotropic strain fields and chemical disorder across interfaces, and their changes with t, define the local structure and hence the spin-polarized electronic structures. If PMA originates from surface MCA alone or predominantly via symmetry breaking, then it must be always present at the transition layer even in thicker layers such as that studied here. However this work presents evidence that in-plane, not perpendicular, anisotropy in m_L exists at the interface of thicker films. As reported in macroscopic studies, misfit strains of Co-rich transition layers can explain the behavior of PMA with t in Co/Pd multilayers without consideration of K_S [12,13]. A major difference in the transition layer studied here and thinner layers exhibiting PMA is misfit strain that depends sensitively on t. This strain effect may be related to the direction of m_L anisotropy, and possibly directly to MA.

It is possible that enhanced spin-orbit interaction and its anisotropy in the transition layer could be influenced by misfit strains [40,41] and indirectly by chemical asymmetry or spin-spin exchange coupling that also play a role in overall MA between layers having different MA [8]. This suggests that the MA may be influenced by anisotropy in coupling interactions, rather than strictly by anisotropy in local crystal fields. This is consistent with the recent suggestion that the anisotropic part of ξ is directly related to MA [42].

In conclusions, the standing wave technique introduced here gives magnetic circular dichroism a much enhanced depth resolution that is applicable to study buried interfaces. As applied to a Pd/Co/Pd trilayer structure, such measurements reveal strong changes in the Co magnetic and electronic structure localized at the buried interface. The modified Co magnetism found in these interfacial transition layers is presumably a precursor to perpendicular magnetic anisotropy, but the large in-plane value of the enhanced orbital moments show that the reorientation transition to perpendicular magnetic anisotropy is very complex, perhaps arising when the Co layer thickness becomes comparable to the transition layer thickness. Further study of this and other problems in interfacial magnetism and interface science in general will benefit from techniques based on soft x-ray standing wave that can provide direct depth resolution at buried interfaces.

Acknowledgments

We thank C. Fadley, G. van der Laan, S. Bader, J. Stöhr, and E. Fulleton for their review and comments, and J. Bowers for assistance in sample preparation. S.K.K is indebted to V. A. Chernov (Novosibirsk, Russia) for stimulating discussion. The MCD measurements were performed on bending magnet beamline 9.3.2 at the Advanced Light Source, Lawrence Berkeley National Laboratory. This work is supported by the Director, Office of Science, Office of Basic Energy Sciences, Materials Sciences Division of the U.S. Department of Energy under Contract No. DE-AC03-76SF00098.

References

1. L. Néel, J. Phys. Rad., **15**, 376 (1954)
2. P. F. Carcia, A. D. Meinhaldt, A. Suna, Appl. Phys. Lett., **47**, 178 (1985)
3. B. N. Engel et al., Phys. Rev. Lett., **67**, 1910 (1991)
4. M. T. Johnson et al., Phys. Rev. Lett., **69**, 3575 (1992)
5. A. Thiaville and J. Miltat, Science, **284**, 1939 (1999)
6. J. Stöhr et al., Science **259**, 658 (1993)
7. D. Weller et al., Phys. Rev. Lett., **75**, 3752 (1995)
8. H. A. Dürr et al., Science, **277**, 213 (1997)
9. H. A. Dürr et al., Science, **284**, 2166 (1999)
10. F. J. A. den Broeder, W. Hoving, P. J. H. Bloemen, Magn. Magn. Mater., **93**, 562 (1991)
11. M. T. Johnson et al., Rep. Prog. Phys., **59**, 1409 (1996)
12. C. H. Lee et al.,Phys. Rev. B **42**, 1066 (1990)
13. S.-K. Kim, V. A. Chernov, Y. M. Koo, J. Magn. Magn. Mater., **170**, L7 (1997)

14. S.-K. Kim et al., Phys. Rev. B **53,** 11 114 (1996)
15. J. G. Gay and R. Richer, Phys. Rev. Lett., **56**, 2728 (1986)
16. P. Bruno, Phys. Rev. B**39**, 865 (1989)
17. O. Eriksson et al., Phys. Rev. B**41**, 11807 (1990)
18. A. J. Freeman and R. Wu, J. Magn. Magn. Mater., **100**, 497 (1991)
19. G. H. Daalderop, P. J. Kelly, F. J. A. den Broeder, Phys. Rev. Lett., **68**, 682 (1992)
20. See, for example, review paper of [11]
21. B. T. Thole et al., Phys. Rev. Lett., **68**, 1943 (1992)
22. P. Carra et al., Phys. Rev. Lett., **70**, 694 (1993)
23. Y. Wu et al., Phys. Rev. Lett., **69**, 2307 (1992)
24. C. T. Chen et al., Phys. Rev. Lett., **75**, 152 (1995)
25. J. Stöhr and H. König, Phys. Rev. Lett., **75**, 3748 (1995)
26. M. G. Samant et al, Phys. Rev. Lett., **72**, 1112 (1994)
27. M. Tisher et al., Phys. Rev. Lett., **75**, 1602 (1995)
28. N. Nakajima et al., Phys. Rev. Lett., **81**, 5229 (1998)
29. H. A. Dürr et al.,Phys. Rev. B **58**, R11 853 (1998)
30. M. J. Bedzyk, G. M. bommarito, M, Caffrey, T. L. Penner, Science, **248**, 52 (1990)
31. Y. L. Qian et al., Science, **265**, 1555 (1994)
32. A. Kazimirov, J. Zegenhagen, M. Cardona, Science, **282**, 930 (1998): A. Kazimirov J. Zegenhagen, M. Cardona, Science, **282**, 930 (1998)
33. Because the Co layer is so thin, possible saturation effects in TEY measurement [R. Nakajima, J. Stöhr, Y. U. Idzerda, Phys. Rev. B**59**, 6421 (1999)] are negligible, as demonstrated in Fig. 1 that shows a large penetration depth compared to electron escape depths
34. S.-K. Kim and J. B. Kortright, unpublished material
35. J. Stöhr, J. Elect. Spect. and Rel. Phen., **75**, 253 (1995)
36. D. Weller et al., Phys. Rev. B**49**, 12 888 (1994)
37. A. S. Chakravarty, Introduction to the Magnetic Properties of Solids, (John Wiley and Sons, New York, USA, 1980), p.66
38. m_S is the result of the imbalance between majority spin-up and minority spin-down electrons, and hence $m_S = (n_h^{\uparrow} - n_h^{\downarrow})$. In the d-electron band picture, it is well known that a band narrowing and enhanced density of states at the Fermi energy may increase the imbalance of the major and minor spins
39. The idea following that angle-averaged m_L remains constant while anisotropy in m_L increases with decreasing t (see Ref.[35]), the large in-plane interfacial enhancement observed here implies a decrease in its perpendicular component.
40. K. Yosida, Theory of Magnetism (Springer-Verlag, Berlin, Germany, 1996)
41. S.-K. Kim, V. A. Chernov, J. B. Kortright, Y. M. Koo, Appl. Phys. Lett., **71**, 66 (1997)
42. G. van der Laan, Phys. Rev. Lett., **82**, 640 (1999)

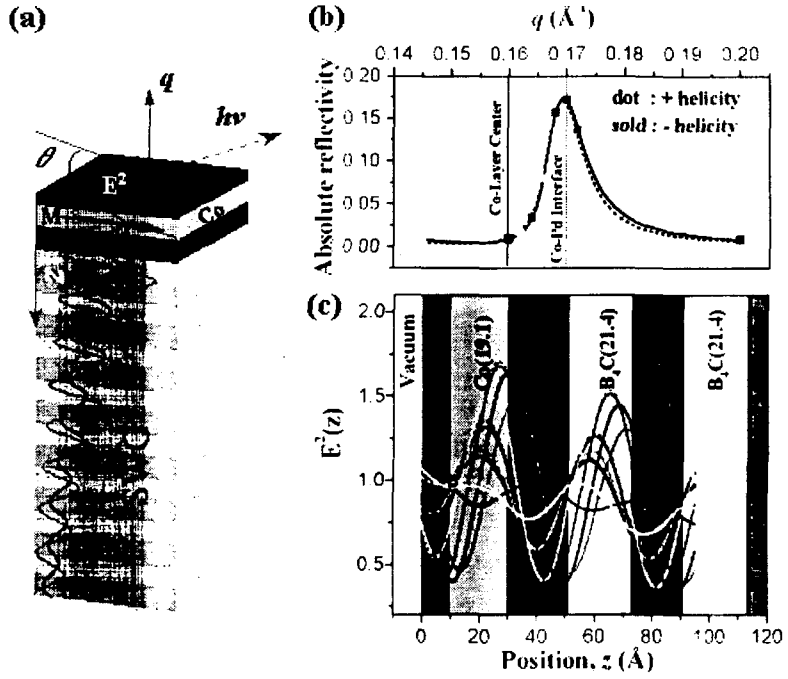

Fig. 1. Experimental geometry including standing wave generator and magnetic trilayer are in (a). Calculated reflectivities at the Co L_3 ($2p_{3/2}$) line versus the scattering vector q in (b). Interference of incident and reflected fields produce standing waves (SW's) versus depth in the magnetic trilayer structure in (c). In each panel, solid and dotted lines refer to opposite helicities, and SW's are calculated at q values indicated by the same color symbol in (b). Absorption signals at a given depth z are proportional to $E^2(z)$ and the variation of $E^2(z)$ with q provides depth resolution. The strong SW at q = 0.17 Å^{-1} much enhances the contribution of interfacial Co atoms as compared those at the center of the Co layer. Differences with helicity in the SW fields result from helicity-dependent Co optical properties, but are very small even at the Co L_3 edge because the Co layer is so thin. The vertical lines in (b) indicate where the anti-node (maximum) of the SW is at the Co/Pd interface (q = 0.17 Å^{-1}) and in the center of the Co layer (q = 0.16 Å^{-1}). Well away from the strong SW modulation, the Co absorption is weighted roughly equally across the layer.

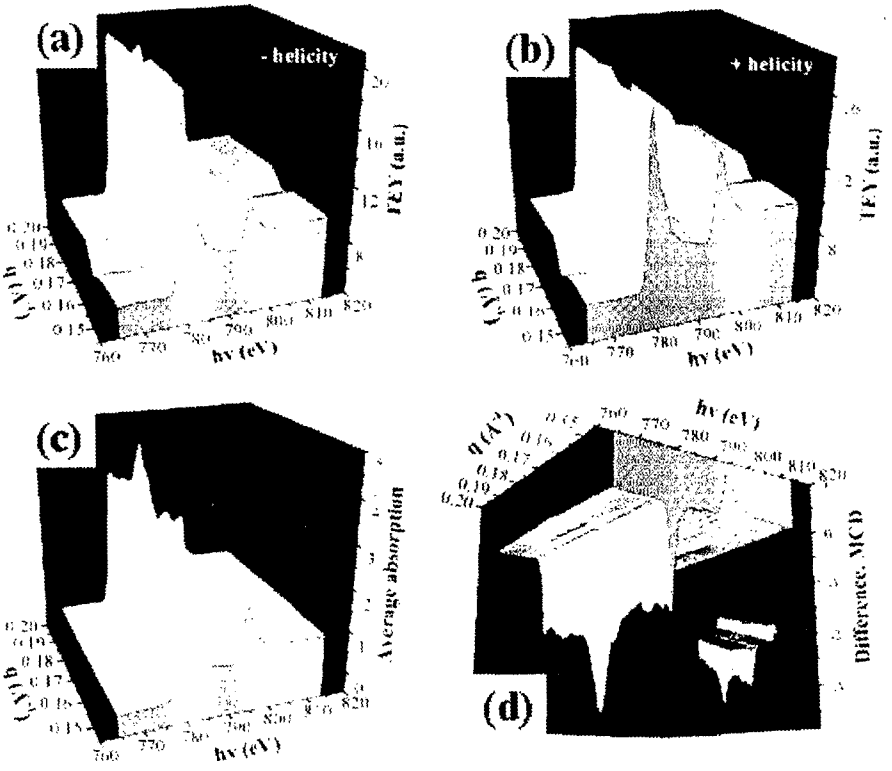

Fig. 2. Total-electron-yield (TEY) absorption spectra on a (q, hv) surface as measured with reversed magnetization in (a) and (b) reveal SW modulations versus q. After normalization of each absorption surface to a per atom scale, their sum and difference yield polarization-averaged and magnetic circular dichroism (MCD) spectral surfaces in (c) and (d), respectively. SW enhancements in these normalized surfaces with q reflect changing absorption with position across the Co layer as weighted by $E^2(z)$.

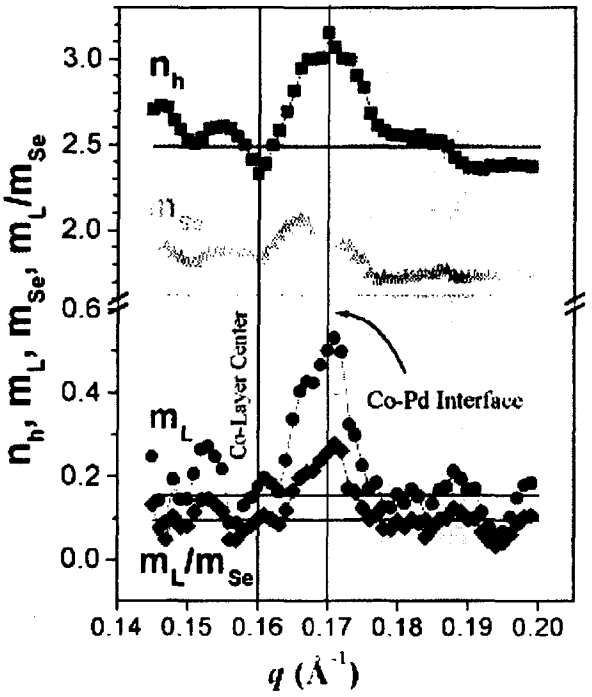

Fig. 3. Based on sum-rule analysis, strong SW enhancements in n_h, m_{Se}, m_L, and m_L / m_{Se} reveal distinctly different electronic and magnetic properties of Co at the interface compared that at the center of the Co layer. The scale of n_h is set by normalizing values in the range outside $0.16 < q < 0.18$ Å^{-1} to the bulk value of 2.49. All straight lines indicate values obtained from a 50-70 Å thick Co film by Chen *et al.*[24].